HHS Public Access

Author manuscript

Int J Radiat Biol. Author manuscript; available in PMC 2016 February 05.

Published in final edited form as:

Int J Radiat Biol. 2015 August ; 91(8): 634–642. doi:10.3109/09553002.2015.1047041.

Role of the bradykinin B2 receptor in a rat model of local heart irradiation

Benjamin J. Lieblong[1], **Vijayalakshmi Sridharan**[2], **Anup K. Srivastava**[1], **Eduardo G. Moros**[3], **Sunil K. Sharma**[2], and **Marjan Boerma**[2]

[1]University of Arkansas for Medical Sciences, Department of Pharmacology and Toxicology, Little Rock, Arkansas

[2]University of Arkansas for Medical Sciences, Division of Radiation Health, Department of Pharmaceutical Sciences, Little Rock, Arkansas

[3]Moffitt Cancer Center and Research Institute, Department of Radiation Oncology, Tampa, Florida

Abstract

Purpose—Radiation-induced heart disease (RIHD) is a delayed effect of radiotherapy for cancers of the chest, such as breast, esophageal, and lung. Kinins are small peptides with cardioprotective properties. We previously used a rat model that lacks the precursor kininogen to demonstrate that kinins are involved in RIHD. Here, we examined the role of the kinin B2 receptor (B2R) in early radiation-induced signaling in the heart.

Materials and methods—Male Brown Norway rats received the B2R-selective antagonist HOE-140 (icatibant) via osmotic minipump from 5 days before until 4 weeks after 21 Gy local heart irradiation. At 4 weeks, signaling events were measured in left ventricular homogenates and nuclear extracts using western blotting and real-time polymerase chain reaction. Numbers of CD68-positive (monocytes/macrophages), CD2-positive (T-lymphocytes), and mast cells were measured using immunohistochemistry.

Results—Radiation-induced c-Jun phosphorylation and nuclear translocation were enhanced by HOE-140. HOE-140 did not modify endothelial nitric oxide synthase (eNOS) phosphorylation or alter numbers of CD2-positive or mast cells, but enhanced CD68-positive cell counts in irradiated hearts.

Conclusions—B2R signaling may regulate monocyte/macrophage infiltration and c-Jun signals in the irradiated heart. Although eNOS is a main target for kinins, the B2R may not regulate eNOS phosphorylation in response to radiation.

Correspondence: Marjan Boerma, Ph.D., Division of Radiation Health, Department of Pharmaceutical Sciences, University of Arkansas for Medical Sciences, 4301 West Markham, Slot 522-10, Little Rock, AR 72205, Phone: 501-686-6599; Fax: 501-686-6057, mboerma@uams.edu.

Declaration of Interest

The authors report no conflicts of interest.

Keywords

bradykinin; B2 receptor; c-Jun; heart; macrophages

Introduction

Radiation therapy (RT) is a leading treatment option for cancer, with estimates that over 50% of patients receive such treatment (DeSantis *et al.* 2014). Patients with thoracic cancers such as lung, breast, and Hodgkin's lymphoma frequently receive radiation therapy either in conjunction with conventional antineoplastics or alone. Adjuvant whole-breast radiation after breast-conserving surgery, for example, has been shown to reduce the risk of local reoccurrences by about two-thirds (Early Breast Cancer Trialists' Collaborative Group 2011). Although RT is useful in decreasing morbidity from such cancers, all or part of the heart can be situated in the field of radiation. As a result, many years after irradiation, signs of cardiac damage present (Darby *et al.* 2010). The resulting pathologies, collectively known as radiation-induced heart disease (RIHD), can lead to the intersection of the two leading causes of morbidity and mortality worldwide: cancer and cardiovascular diseases (Fuster and Voûte 2005).

RIHD can manifest itself in a diverse array of symptoms such as accelerated atherosclerosis, conduction abnormalities, valvular defects, and cardiac remodeling (Jaworski *et al*. 2013). For instance, of 116 patients treated with mediastinal radiotherapy for Hodgkin's disease, 31% showed moderate valvular regurgitation 10 years after therapy, mostly in the mitral and aortic valves (Wethal *et al*. 2009). Abnormalities in the conduction system post-RT are frequently observed; including atrioventricular block, prolonged QT interval, supraventricular arrhythmia, and ventricular tachycardia (Heidenreich and Kapoor 2009; Larsen *et al.* 1992). In addition, diffuse interstitial fibrosis occurs in the heart after it receives relatively low doses of radiation, and as a result, the compliance of the heart is altered (Nellessen *et al.* 2010). Cardiac fibrosis may contribute to both systolic and diastolic dysfunction, the latter of which is associated with stress-induced ischemia (Heidenreich and Kapoor 2009).

RIHD does not present until many years have passed since the heart was irradiated (Cuzick *et al.* 1994). Because the symptoms of RIHD do not present for many years after RT, long-term cancer survivors are a particularly vulnerable subset of patients in developing RIHD. Additional factors, such as greater exposure of the heart, younger age at the time of RT, and even concomitant use of cardiotoxic chemotherapeutics such as anthracyclines and maybe even trastuzumab can hasten or worsen RIHD (Keefe 2003; Demirci *et al.* 2009). Despite the progressive nature of RIHD, there are no pharmacological treatments, interventions, or prophylaxes approved for clinical use.

Bradykinin is a peptide hormone with cardioprotective actions in many heart and cardiovascular diseases (Regoli *et al.* 2012). In the kallikrein-kinin system (KKS), bradykinin and other kinins are products of the proteolytic cleavage of low- and high-molecular weight kininogen by tissue and plasma kallikrein and also mast cell-derived proteases (Imamura *et al.* 1996). Kinins interact with either of two known receptors, both of

which are G-protein coupled receptors: the constitutively expressed B2 receptor, and the stress-inducible B1 receptor (Marceau 1998). Classically, kinins are known for their involvement in inflammatory processes. Activation of the B2 receptor can lead to various signal transduction pathways culminating in the release of cytokines and other inflammatory mediators (Marceau 1983). Another major B2 receptor-mediated intracellular signaling event is the phosphorylation and activation of endothelial nitric oxide synthase (eNOS) and the induction of prostacyclin, mediating cardioprotective effects through vasodilation and inhibition of cardiac fibroblasts (Kim *et al.* 1999; Jones and Bolli 2006). These and other effects imply that targeting bradykinin or the kallikrein-kinin system could be therapeutic in a wide range of disease states. Not surprisingly, angiotensin converting enzyme inhibitors (which inhibit the degradation of bradykinin) are first-line treatments in a variety of cardiovascular conditions, ranging from hypertension to post-myocardial infarction prophylaxis (Böhm *et al.* 2010).

Brown Norway Katholiek (BN/Ka) rats carry a point mutation in the kininogen gene, leading to the defective secretion of kininogen, and thus these animals lack circulating kinins (Damas 1996). We previously have shown that BN/Ka rats exhibited exacerbations of certain inflammatory manifestations of RIHD compared to wild type Brown Norway (BN) rats (Sridharan *et al.* 2012). Moreover, while in BN rats radiation induced phosphorylation of extracellular signal-regulated kinase (Erk) 1/2, a mitogen-activated protein kinase known for its beneficial effects in the heart (Das *et al.* 2009), Erk 1/2 phosphorylation was not observed in BN/Ka animals. Similarly, kininogen-deficiency prevented radiation-induced phosphorylation of c-jun, a transcription factor that has recently been shown to reduce adverse cardiac remodeling (Windak *et al.* 2013). Here, we investigate the role of the B2 receptor in signaling events and inflammatory infiltration leading up to adverse remodeling in the irradiated heart by blocking the receptor pharmacologically using the bradykinin analog, HOE-140 (icatibant), a B2 receptor-selective antagonist (Wirth *et al.* 1991).

Materials and methods

Assessment of long-term stability of HOE-140 in solution at 37°C

To determine whether HOE-140 may be delivered via osmotic minipumps, its long-term stability in saline vehicle at 37°C was assessed. HOE-140 (1 mg/mL in 0.9% saline) was placed in osmotic minipumps (Model 2002, Alzet, Palo Alto, CA, USA) and incubated at 37°C to mimic *in vivo* conditions. Aliquots were collected and analyzed by high-performance liquid chromatography (HPLC) immediately after dissolving HOE-140 and after 5, 6, 8, 13, and 14 days of incubation in a minipump. Each sample was diluted 1:100 in Mobile Phase A (0.1% trifluoroacetic acid (TFA) in HPLC-grade H_2O). Diluted samples were injected (20 μL) onto a Shimadzu LC-10AP HPLC system (Columbia, MD, USA) and resolved using a 150x4.60 mm reversed-phase Luna 5 μm C18 column (Phenomenex, Torrance, CA, USA) heated to 100ºC. A gradient method effectively eluted HOE-140 at a flow rate of 1 mL/min. The mobile phase consisted of (A) H_2O (0.1% TFA) and (B) acetonitrile (0.1% TFA) with 100% A and 0% B initially, followed by a linear gradient from 0 to 35% B (0-20min). Elution of HOE-140 was monitored by ultraviolet (UV) absorbance at 210nm.

In vivo study design

All procedures in this study were approved by the Institutional Animal Care and Use committee of the University of Arkansas for Medical Sciences. A total of 47 male BN rats weighing 260-280g were obtained from Harlan (Indianapolis, IN, USA) and housed on a 12h:12h light:dark cycle with *ad libitum* access to food and water. A dose of 0.5 mg/kg body weight/day HOE-140 (Tocris, Bristol, UK) or vehicle (0.9% saline) was administered subcutaneously at 0.49 μL/hr via osmotic minipump (Model 2002, Alzet). Minipumps filled with either HOE-140 or saline were subcutaneously implanted under 3% isoflurane anesthesia via an incision in between the scapulae. First, in order to verify that 0.5 mg/kg/day HOE-140 administered via osmotic minipumps induces B2 receptor blockade at the functional level, 14 animals treated with HOE-140 or vehicle (n=7) were observed for latency to hypotensive response to exogenous bradykinin as described below, using a protocol adapted from Bao *et al.* (1992). Then, a separate group of animals continuously received HOE-140 or saline vehicle from 5 days before receiving 21 Gy local heart irradiation until sacrifice at 4 weeks after irradiation. To achieve 4 weeks of treatment, pre-primed minipumps containing freshly dissolved HOE-140 were reimplanted after 2 weeks. Thus, the following four groups were analyzed using the remaining 33 animals: (1) Sham-irradiated + vehicle, (2) Sham-irradiated + 0.5 mg/kg/day HOE-140, (3) 21 Gy, and (4) 21 Gy + 0.5 mg/kg/day HOE-140. To sacrifice at 4 weeks post-irradiation, rats were anesthetized with 3% isoflurane, and hearts were isolated and sliced to form two coronal sections: one half for histological analyses, and small aliquots of the other half were immediately snap frozen for later molecular analyses (western blotting and real-time polymerase chain reaction (PCR)) as described below.

Verification of B2 receptor blockade by HOE-140 in response to exogenous bradykinin

HOE-140, a bradykinin receptor antagonist, blocks the hypotensive effect of bradykinin. At time points between 4 and 32 days after implantation of a minipump containing either HOE-140 (0.5 mg/kg/day) or saline vehicle, rats were anesthetized with 2.5% isoflurane anesthesia and the right femoral artery and vein were isolated and dissected away from the femoral nerve. A heparinized saline-filled catheter composed of PE-50 tubing connected to a pressure transducer (Model SP 844, Memscap, Skoppum, Norway) was inserted in the thoracic aorta via the cannulated femoral artery. Aortic blood pressure was measured real-time using the PowerLab 4/35 system and LabChart software (ADInstruments, Colorado Springs, CO, USA). A second catheter was inserted in the caudal vena cava via the cannulated femoral vein for intravenous administration of bradykinin. Blood pressure readings were allowed to stabilize for about 5 minutes, after which point a baseline infusion of 1.0 mL saline was administered at 2 mL/minute. To then verify that HOE-140 induced a B2 receptor blockade at the functional level, 1.0 mL of bradykinin (Tocris) solution in physiological saline was infused at a rate of 2 mL/min to a total dose of 0.3 μg/kg body weight. For data analysis, mean arterial pressure (MAP) was calculated from raw blood pressure readings.

Animal model of local heart irradiation

Animals received local irradiation to the heart using the Small Animal Conformal Radiation Therapy Device (SACRTD) developed at our institution and previously described (Sridharan *et al.* 2013). In brief, the SACRTD consists of a 225 kVp X-ray source (GE Isovolt Titan 225, General Electric, Fairfield, CT, USA) mounted on a custom made "gantry", a stage mounted on a robotic arm positioning system (Viper™ s650 Adept Technology, Pleasanton, CA, USA), and a flat panel digital X-ray detector of 200 μm resolution (XRD 0820 CM3 Perkin Elmer, Fremont CA, USA). For the purpose of local heart irradiation, a brass and aluminum collimating assembly was attached to the X-ray tube to produce a field of 19 mm diameter at the isocenter. Rats were anesthetized with 3% isoflurane and placed vertically in a Plexiglas holder with no barriers between the radiation beam and the chest. The heart was exposed in three 19 mm-diameter fields (one anterior-posterior and two lateral fields perpendicular to the first) of 7 Gy each (225 kV, 13 mA, 0.5 mm Cu-filtration, resulting in 1.92 Gy/min at 1 cm tissue depth). Before each exposure, the location of the heart was verified with the X-ray detector (70 kV, 5 mA, <1 cGy) and, when necessary, the position of the rat was adjusted with the use of the robotic arm. The implanted osmotic minipumps were located outside the fields of radiation at all times.

Nuclear extract preparation

At sacrifice, pieces of left ventricular tissue were excised and snap-frozen. These frozen tissue specimens (approximately 50-80 mg) were used to prepare nuclear extracts using the ActiveMotif (Carlsbad, CA, USA) kit and protocol with the following modifications. Tissues were homogenized in 2.0 mL 1X hypotonic buffer using 50 strokes motorized Dounce homogenization. After 10 min incubation at 4°C, homogenates were spun at 850g at 4°C for 10 minutes to pellet nuclei. After discarding the supernatant, the pellet of nuclei was washed by resuspending in 1X hypotonic buffer, and then incubated at 4°C for 10 minutes. Then, 50μL detergent was added to each sample, vortexed at maximum speed for 90 sec, and then spun 14,000g at 4°C for 1 min. After discarding the supernatant and washing in phosphate-buffered saline, the pellet was lysed in radioimmunoprecipitation assay (RIPA) buffer containing protease and phosphatase inhibitors (both 10μL/mL, Sigma-Aldrich, St. Louis, MO, USA). After resuspension, samples were sonicated for two 6-second cycles, and then incubated rocking at 4°C for 30 minutes. Finally, samples were spun 14,000g at 4°C for 10 minutes, and the nuclear extract supernatant was decanted. Nuclear extract protein concentration was estimated using a bicinchoninic acid (BCA) assay (Thermo Scientific, Rockford, IL, USA) for western blot analysis. The purity of all nuclear extracts was verified with western blots for the nuclear marker Lamin-B and the cytoplasmic protein glyceraldehyde-3-phosphate dehydrogenase (GAPDH), with methods described below (representative results are shown in Supplemental Figure 2).

Total left ventricular homogenization

Snap-frozen tissue samples were homogenized in RIPA buffer containing protease and phosphatase inhibitors (both 10μL/mL, Sigma-Aldrich). After 50 strokes using a motorized Dounce homogenizer, homogenates were spun at 20,000g at 4°C for 15 minutes, and the

supernatant protein concentration was estimated using a BCA assay (Thermo Scientific) for western blot analysis.

Western blotting

Protein samples of nuclear extracts or total left ventricular homogenates were prepared from frozen tissue aliquots as described above, and then boiled for 4 minutes in Laemmli sample buffer containing β-mercaptoethanol (1:20 vol/vol). Samples were then separated in Mini-Protean TGX™ polyacrylamide gels (Bio-Rad, Hercules, CA, USA) at 90V and transferred to polyvinylidene difluoride membranes at 20V overnight at 4°C. Non-specific antibody binding was reduced by tris-buffered saline (TBS) containing 0.05% Tween-20 and 5% dry powdered milk. Membranes were incubated at 4°C overnight with the following primary antibodies: rabbit anti-phospho Erk 1/2 (Cell Signaling, Danvers, MA, USA), rabbit anti-Erk 1/2 (Cell Signaling), goat anti-phospho eNOS at S1177 (Santa Cruz Biotechnology, Dallas, TX, USA), rabbit anti-eNOS (Santa Cruz Biotechnology), rabbit anti-phospho c-Jun at Ser63 (Cell Signaling), rabbit anti-phospho c-Jun at Ser73 (Cell Signaling), rabbit anti-c-Jun (Cell Signaling), mouse anti-GAPDH (Sigma-Aldrich), and goat anti-Lamin-B (Santa Cruz Biotechnology). Primary antibodies were followed by 1 hour incubation with the appropriate of the following horseradish peroxidase-conjugated immunoglobulin G (IgG) secondary antibodies: goat anti-rabbit, goat anti-mouse, and rabbit anti-goat (all Santa Cruz Biotechnology). Antibody binding was visualized with ECL Plus Western Blotting Detection reagent (GE Healthcare Life Sciences, Uppsala, Sweden) on CL-Xposure Film (Thermo Scientific). Films were scanned using an AlphaImager gel documentation system (Protein Simple, Santa Clara, CA, USA) and protein bands were quantified using the public domain software ImageJ.

Histochemical staining for collagen and mast cells

At sacrifice, coronal sections of hearts were fixed in formalin or methanol Carnoy's solution (60% methanol, 30% chloroform, 10% acetic acid) overnight, then later embedded in paraffin, cut into 5μm sections, and then deparaffinized and rehydrated for staining. For collagen staining, sections were incubated in Picrosirius red (American MasterTech, Lodi, CA, USA) with 0.01% w/v Fast Green (Fisher Scientific, Waltham, MA, USA) for 2 hours. Sections were scanned with a ScanScope CS2 slide scanner and analyzed with ImageScope 12 software (Aperio, Vista, CA, USA). The relative collagen area was calculated as the area stained positive with Picrosirius red divided by the total tissue area. For determination of mast cell numbers, sections were incubated in 0.5% Toluidine Blue in 0.5N HCl for 72 hours, followed by 0.7N HCl for 10 minutes. Eosin was used as a counterstain. Total numbers of mast cells were counted for each section in a blinded fashion.

Immunohistochemical detection of macrophages/monocytes and T-lymphocytes

At sacrifice, hearts were fixed in formalin or methanol Carnoy's solution (60% methanol, 30% chloroform, 10% acetic acid) overnight, then later embedded in paraffin, and cut into 5μm sections for immunohistochemistry. Formalin-fixed sections were subjected to antigen retrieval by a 5-minute incubation at 37°C in Proteinase K (Dako, Carpinteria, CA, USA), diluted 1:50 v/v in 50mM Tris-HCl, pH 7.6. In all sections, endogenous peroxidases were blocked with 1% H_2O_2 in methanol. Nonspecific binding was blocked with a buffer

containing 10% normal horse or donkey serum, 3% non-fat dry milk, and 0.1% bovine serum albumin. Formalin-fixed sections were incubated in primary mouse anti-CD68 (1:100, Santa Cruz Biotechnology), and methanol Carnoy's-fixed sections were incubated in mouse anti-CD68 (1:100, Abcam, Cambridge, MA, USA), or mouse anti-CD2 (Cedarlane, Burlington, NC, USA), all diluted in TBS and incubated overnight at 4°C. Each primary antibody was followed by horse-anti mouse IgG (1:400, Vector Laboratories, Burlingame, CA, USA) or donkey anti-mouse IgG (1:400, Vector Laboratories) diluted in TBS, and an avidin-biotin peroxidase complex (Vector Laboratories). All immunostainings were visualized with 0.5 mg/mL 2,2-diaminobenzidine tetrahydrochloride (Sigma-Aldrich) and 0.003% H_2O_2 in TBS. Hematoxylin was used as a counterstain. Total numbers of CD68 positive ($CD68^+$) cells and CD2-positive ($CD2^+$) cells were counted for each section in a blinded fashion.

Real-time quantitative PCR

At sacrifice, aliquots of left ventricular tissue were excised and snap-frozen. For the purpose of real-time PCR, frozen pieces of left ventricular tissue were homogenized in Ultraspec RNA reagent (Biotecx Laboratories, Houston, TX, USA). After treatment with RQ-DNAse I (Promega, Madison, WI, USA) at 37°C for 30 minutes, followed by DNAse inactivation at 75°C for 10 minutes, complementary DNA (cDNA) was synthesized using the High Capacity cDNA Archive Kit (Life Technologies, Grand Island, NY, USA). Relative mRNA expression was assessed with real-time quantitative PCR (TaqMan) using the 7500 Fast Real-Time PCR System and the following predesigned assays for rat: B1 receptor (Rn02064589_s1), B2 receptor (Rn00597384_m1), 18S rRNA (Hs99999901_s1), and angiotensin II type 2 (AT_2) receptor (Rn00560677_s1; all Life Technologies). Relative mRNA levels were calculated according to the delta delta Ct method, using 18S rRNA as a normalizer. Samples of cDNA prepared from total rat brain, using the same Ultraspec-based protocol as above, were selected for use as a positive control for the B1, B2, and AT_2 receptors.

Statistical analysis

Data were evaluated with the software package NCSS 8 (NCSS, Kaysville, UT, USA). Data were analyzed with two-way Analysis of Variance (ANOVA), followed by Newman-Keuls individual comparisons. Data are reported as average ± standard error of the mean (SEM). The criterion for significance was a $p<0.05$.

Results

Characterization of B2 receptor blockade with HOE-140

This study investigated the role of the B2 receptor in radiation-induced alterations in the heart at times leading up to adverse remodeling. To accomplish this, HOE-140 was continuously infused at 0.5 mg/kg/day from 5 days before irradiation until sacrifice 28 days after irradiation. To validate that HOE-140 retained chemical stability for this period of time, osmotic minipumps containing 1 mg/mL HOE-140 were incubated at 37°C to mimic *in vivo* conditions. Aliquots of HOE-140 taken from minipumps were subjected to HPLC analysis, and no significant degradation was observed (Figure 1). To validate that HOE-140

will act at its molecular target for the intended duration of the *in vivo* experiments, an *in vivo* functional assay was used. In animals implanted with vehicle-containing osmotic minipumps, bradykinin (0.3 μg/kg infusion for 30 sec.) caused a decrease in MAP from 75.4 mmHg ± 1.1 at initial baseline to 70.1 mmHg ± 1.3 at the end of bradykinin infusion (p=0.016). In animals implanted with HOE-140-containing osmotic minipumps, bradykinin (0.3 μg/kg infusion) caused a small but non-significant decrease in MAP from 76.8 mmHg ± 1.7 initially, to 75.7 mmHg ± 1.6. Hence, treatment with HOE-140 in osmotic minipumps blocked the response to exogenous BK (Figure 2). This functional inhibition of the B2 receptor was observed as early as after 4 days of HOE-140 treatment and as late as 32 days of HOE-140 treatment. Baseline MAP was not altered by HOE-140 treatment (Supplemental Figure 1).

Because prolonged B2 blockade may cause a compensatory upregulation of B1, B2, or AT_2 receptors, we determined the expression of these receptors at the endpoint of our experiment. Compared to B2 receptor mRNA expression in sham animals (1.07 ± 0.09), B2 receptor mRNA expression was not altered by HOE-140 alone (0.86 ± 0.31), 21 Gy irradiation alone (0.86 ± 0.16), or radiation and HOE-140 in combination (1.15 ± 0.30). No changes were observed in the expression of the B2 receptor, and B1 and AT_2 receptor expression remained undetectable (data not shown).

Cardiac histology and inflammatory infiltration at 4 weeks after irradiation

At 4 weeks after irradiation, there were no significant changes in left ventricular collagen deposition or T-lymphocyte numbers, indicating that this is a time point leading up to late adverse remodeling (data not shown). As shown by us previously at this time point, radiation caused a 3-fold reduction in cardiac mast cell numbers. Mast cell numbers were not modified by HOE-140 treatment (Figure 3A). HOE-140 treatment caused an increase in myocardial infiltration of $CD68^+$ cells in irradiated hearts, while neither HOE-140 nor irradiation alone changed $CD68^+$ cell infiltration (Figure 3B). Representative micrographs for CD68 immunohistochemistry and mast cell staining are shown in Supplemental Figure 3.

Effects of B2 receptor blockade on molecular pathways 4 weeks after irradiation

Erk 1/2, c-Jun, and eNOS are three main targets for bradykinin signaling. At the 4 weeks time point, radiation caused an increase in eNOS phosphorylation, which was not modified by HOE-140 treatment (Figure 4). HOE-140 caused a two-fold reduction in phosphorylation of Erk 1/2 in the sham animals, but not in irradiated animals (Figure 5). In left ventricular total homogenates, radiation caused an increase in c-Jun phosphorylation at both the Ser73 and Ser63 residues, the latter of which was enhanced by HOE-140 (Figure 6A). The increase in c-Jun phosphorylation after irradiation coincided with an approximate 2.5-fold increase in nuclear c-Jun, which was further increased by HOE-140 treatment (Figure 6B). Related representative western blots are shown in Supplemental Figures 4-6.

Discussion

RIHD as a human condition is a delayed effect of thoracic RT; cardiac functional deficits frequently do not present until 10 or more years after receiving RT. Although some rat strain

and radiation dose dependencies exist, rats in our model of local heart irradiation tends to develop signs of RIHD, such as fibrosis, around 3 months after single-fraction X-irradiation, and these appear to be progressive (Boerma *et al.* 2004). In this 1-month study, our interests were in the earlier signaling events that occur leading up to adverse remodeling associated with the later time points post-irradiation. By using a genetic animal model, we previously demonstrated that cardiac infiltration of inflammatory cells at 6 months after receiving local heart irradiation is modified, at least in part, by the KKS (Sridharan *et al.* 2012). Here, we present data suggesting that the B2 receptor, the main receptor for KKS mediators in the heart, may play an inhibitory role in monocyte/macrophage infiltration in the heart in response to radiation. On the other hand, radiation-induced eNOS phosphorylation and its early effect on mast cell numbers may not be regulated by the B2 receptor.

Our previous studies with kininogen-deficient rats involved local heart doses of 18 Gy and 24 Gy, to detect potential radiation dose-dependent effects (Sridharan *et al.* 2012). In the current study we were limited to one radiation dose. Because in our previous studies a single dose of 18 Gy caused only mild effects in the heart, and a single dose of 24 Gy is generally considered a high dose in animal models of local heart irradiation, we here elected to use an intermediate radiation dose of 21 Gy. We have previously shown that it produces moderate cardiac radiation injury in the rat, similar to fractionated schedules as also used in our laboratory (Boerma *et al.* 2008).

The best-described B2 receptor antagonist, HOE-140, has been used in many animal models, and has even reached clinical use to relieve acute swelling attacks in hereditary angioedema patients (Bork *et al.* 2007). Its *in vivo* use in a chronic dosing paradigm is more difficult, owing to its short elimination half-life (about 1.8 hours in humans (Cockcroft *et al.* 1994)) and lack of oral bioavailability, as is expected with a peptide drug. Our HPLC technique demonstrated no loss of HOE-140 within osmotic minipumps within 16 days (the duration that osmotic minipumps would dispense HOE-140 in our experiments). Next, we assessed whether this delivery technique would indeed block its molecular target, the B2 receptor, *in vivo*. A functional inhibition of the hypotensive response to exogenously administered BK implied that our dosing paradigm of HOE-140 blocked the B2 receptor at the functional level. HOE-140 did not alter baseline (i.e., before infusion of BK) MAP. Thus, changes in the heart due to potential activity of HOE-140 on peripheral vascular tone can be excluded.

Although the intended consequence of HOE-140 treatment is to block the signaling of endogenous kinins, such treatment has the potential to induce receptor modulation. Various receptors are upregulated in response to antagonism, perhaps as a cellular compensatory mechanism (Wonnacott 1990). Furthermore, the presence of 2 BK receptors with similar signaling motifs implies that antagonism of one receptor could induce the expression of the other. Moreover, studies have demonstrated a cross-talk between the receptors of the renin-angiotensin system and the KKS, and overexpression of the AT_2 receptor activates the B2 receptor (Tsutsumi *et al.* 1999). Both the B1 and AT_2 receptor may play compensatory cardioprotective roles in B2 receptor knockout mice (Xu *et al.* 2013). We therefore examined whether HOE-140 treatment may modulate the B1, B2, or AT_2 receptors and confirmed that our 4 weeks treatment with HOE-140 was not associated with any compensatory changes in the expression of these receptors.

The best-characterized downstream effect of BK signaling is the activation of eNOS, the major source of vasodilatory NO in the vascular endothelium. The eNOS enzyme itself has dynamic regulation due to its many phosphorylation sites, each of which confer varying degrees of activation or inhibition, and therefore modulate NO generation (Mount *et al.* 2007). Specifically, eNOS has been shown to be phosphorylated at Ser^{1177} by Akt (Fulton *et al.* 1999), which is a known target of BK signaling (Bae *et al.* 2003; Bell *et al.* 2002). Phosphorylation at this site increases eNOS activity (Fulton *et al.* 1999). In our study, we showed that local heart irradiation caused a 3-fold increase in eNOS phosphorylation at Ser^{1177}, but this was not modified by treatment with HOE-140. Hence, we believe that radiation may induce eNOS phosphorylation at this residue through a pathway independent of B2 receptor signaling. The role of the B2 receptor in radiation-induced phosphorylation of eNOS at other residues remains to be determined.

Although its cellular targets are numerous, activation of Erk 1/2 in the heart favors survival and enhanced contractility (Rose *et al.* 2010). Erk 1/2 is an established target of BK signaling, thus corroborating our decrease in Erk 1/2 phosphorylation with HOE-140 treatment in animals without irradiation. While we have previously shown increased Erk 1/2 phosphorylation at 3 and 6 months after irradiation (Sridharan *et al.* 2012), radiation did not induce Erk 1/2 phosphorylation in the current 1-month study, indicating that radiation-induced Erk 1/2 phosphorylation is a time-dependent process. Interestingly, local heart irradiation did prevent HOE-140 from reducing Erk 1/2 phosphorylation, suggesting that upon irradiation other signaling pathways may “overrule” B2 receptor signaling in regulating the phosphorylation status of Erk 1/2.

Another target of BK signaling is the protein c-Jun, which upon phosphorylation of its activation domain can heterodimerize to form the activator protein-1 (AP-1) transcription factor complex, which regulates cellular proliferation and apoptosis at the transcriptional level (Bohmann *et al*. 1987). c-Jun has recently been shown to prevent myocardial fibrosis and cardiomyocyte apoptosis in cardiac adverse remodeling (Windak *et al.* 2013). The kinases classically associated with c-Jun phosphorylation belong to the c-Jun N-terminal kinase (JNK) family, although c-Jun can also be phosphorylated through Erk 1/2 signaling (Leppä *et al.* 1998). The radiation-induced increase in c-Jun phosphorylation did not coincide with any increase in Erk 1/2 phosphorylation; thus we believe that this event occurs independently of Erk 1/2 signaling. However, HOE-140 treatment in the irradiated hearts caused a further increase in c-Jun phosphorylation at Ser63, implying that BK signaling may regulate c-Jun phosphorylation, perhaps through another kinase than Erk 1/2. Because phosphorylation of c-Jun favors nuclear translocation and subsequent regulation of gene expression (Binetruy *et al.* 1991), we examined levels of c-Jun in nuclear extracts to determine whether the observed c-Jun phosphorylation had a functional consequence. Indeed, we verified that radiation caused nuclear translocation of c-Jun which was further increased by HOE-140 in irradiated animals, suggesting that B2 receptor signaling could inhibit radiation-induced c-Jun signaling.

We have previously shown that the KKS modulates inflammatory infiltration in response to local heart irradiation (Sridharan *et al.* 2012). Interestingly, many immune cells themselves are known to express BK receptors, mast cells and monocytes/macrophages included

(Böckmann and Paegelow 2000). We have previously shown that local heart irradiation in the rat caused a reduction in cardiac mast cell numbers at earlier time points, followed by an increase at later time points when adverse remodeling is apparent (Boerma *et al.* 2004). We here show once more reduced mast cell numbers at 4 weeks after local heart irradiation. HOE-140 did not modify mast cell numbers, suggesting that the B2 receptor is not involved in the early response of mast cells to irradiation. On the other hand, HOE-140 treatment caused an upregulation in the number of $CD68^+$ cells, implying that the B2 receptor has an inhibitory role in monocyte/macrophage infiltration in the irradiated heart. Although kinins are well-known for their pro-inflammatory signaling, many studies have shown kinins to have anti-inflammatory properties (Wang *et al.* 2009). Because monocytes and macrophages express B2 receptors, HOE-140 may have directly modified their proliferation and/or migration. However, due to the complex heterogeneity of macrophage phenotypes (Martinez and Gordon 2014), we cannot exclude that a more complex regulation exists.

In conclusion, the results of these studies indicate that administration of HOE-140 with osmotic minipumps can be used to induce long-term inhibition of the B2 receptor in a rat model. Radiation-induced phosphorylation of eNOS was not modified by HOE-140. On the other hand, while the B2 receptor seems to be involved in the regulation of Erk 1/2 phosphorylation in the unirradiated heart, at 4 weeks after local heart irradiation the role of the B2 receptor may be diminished. Radiation-induced c-Jun phosphorylation and nuclear translocation are both increased with B2 receptor blockade. Lastly, the B2 receptor appears to play an inhibitory role on monocyte/macrophage infiltration or proliferation in the irradiated heart.

Supplementary Material

Refer to Web version on PubMed Central for supplementary material.

Acknowledgements

The authors would like to acknowledge Howard Hendrickson, Ph.D. for his technical assistance with the HPLC studies.

This work was supported by grant funding from the National Institutes of Health (CA148679) and American Cancer Society (RSG-10-125-01-CCE).

References

Bae SW, Kim HS, Cha YN, Park YS, Jo AS, Jo I. Rapid increase in endothelial nitric oxide production by bradykinin is mediated by protein kinase A signaling pathway. Biochem Biophys Res Commun. 2003; 306:981–987. [PubMed: 12821139]

Bao G, Gohlke P, Qadri F, Unger T. Chronic kinin receptor blockade attenuates the antihypertensive effect of ramipril. Hypertension. 1992; 20:74–79. [PubMed: 1319960]

Bell RM, Yellon DM. Bradykinin limits infarction when administered as an adjunct to reperfusion in mouse heart: the role of PI3K, Akt, and eNOS. J Molec Cell Cardiol. 2002; 35:185–193. [PubMed: 12606259]

Binetruy B, Smeal T, Karin M. Ha-ras augments c-Jun activity and stimulates phosphorylation of its activation domain. Nature. 1991; 351:122–127. [PubMed: 1903181]

Böckmann S, Paegelow I. Kinins and kinin receptors: importance for the activation of leukocytes. J Leukoc Biol. 2000; 68:587–592. [PubMed: 11073095]

Boerma M, Zurcher C, Esveldt I, Schutte-Bart CI, Wondergem J. Histopathology of ventricles, coronary arteries and mast cell accumulation in transverse and longitudinal sections of the rat heart after irradiation. Oncol Rep. 2004; 12:213–219. [PubMed: 15254680]

Boerma M, Roberto KA, Hauer-Jensen M. Prevention and treatment of functional and structural radiation injury in the rat heart by pentoxifylline and alpha-tocopherol. Int J Radiat Oncol Biol Phys. 2008; 72:170–177. [PubMed: 18632215]

Böhm M, Baumhäkel M, Mahfoud F, Werner C. From evidence to rationale: cardiovascular protection by angiotensin II receptor blockers compared with angiotensin-converting enzyme inhibitors. Cardiology. 2010; 117:163–173. [PubMed: 21051889]

Bohmann D, Bos TJ, Admon A, Nishimura T, Vogt PK, Tijan R. Human proto-oncogene c-jun encodes a DNA binding protein with structural and functional properties of transcription factor AP-1. Science. 1987; 238:1386–1392. [PubMed: 2825349]

Bork K, Frank J, Grundt B, Schlattmann P, Nussberger J, Kreuz W. Treatment of acute edema attacks in hereditary angioedema with a bradykinin receptor-2 antagonist (Icatibant). J Allergy Clin Immunol. 2007; 119:1497–1503. [PubMed: 17418383]

Cockcroft JR, Chowienczyk PJ, Brett SE, Bender N, Ritter JM. Inhibition of bradykinin-induced vasodilation in human forearm vasculature by icatibant, a potent B2-receptor antagonist. Br J Clin Pharmacol. 1994; 38:317–321. [PubMed: 7833220]

Cuzick J, Stewart H, Rutqvist L, Houghton J, Edwards R, Redmond C, Peto R, Baum M, Fisher B, Host H. Cause-specific mortality in long-term survivors of breast cancer who participated in trials of radiotherapy. J Clin Oncol. 1994; 12:447–453. [PubMed: 8120544]

Darby SC, Cutter DJ, Boerma M, Constine LS, Fajardo LF, Kodama K, Mabuchi K, Marks LB, Mettler FA, Pierce LJ, Trott KR, Yeh ETH, Shore RE. Radiation-related heart disease: current knowledge and future prospects. Int J Radiat Oncol Biol Phys. 2010; 76:656–665. [PubMed: 20159360]

DeSantis CE, Lin CC, Mariotto AB, Siegel RL, Stein KD, Kramer JL, Alteri R, Robbins AS, Jemal A. Cancer treatment and survivorship statistics, 2014. CA Cancer J Clin. 2014; 64:252–271. [PubMed: 24890451]

Early Breast Cancer Trialists' Collaborative Group (EBCTCG). Effect of radiotherapy after breast-conserving surgery on 10-year recurrence and 15-year breast cancer death: meta-analysis of individual patient data for 10 801 women in 17 randomised trials. Lancet. 378:1707–1716.

Damas J. The brown Norway rats and the kinin system. Peptides. 1996; 17:859–872. [PubMed: 8844778]

Das A, Salloum FN, Xi L, Rao YJ, Kukreja RC. ERK phosphorylation mediates sildenafil-induced myocardial protection against ischemia-reperfusion injury in mice. Am J Physiol Heart Circ Physiol. 2009; 296:H1236–H1243. [PubMed: 19286961]

Demirci S, Nam J, Hubbs JL, Nguyen T, Marks LB. Radiation-induced cardiac toxicity after therapy for breast cancer: interaction between treatment era and follow-up duration. Int J Radiat Oncol Biol Phys. 2009; 73:980–987. [PubMed: 19251085]

Fulton D, Gratton J-P, McCabe TJ, Fontana J, Fujio Y, Franke T, et al. Regulation of endothelium-derived nitric oxide production by the protein kinase Akt. Nature. 1999; 399:597–601. [PubMed: 10376602]

Fuster V, Voûte J. MDGs: chronic diseases are not on the agenda. Lancet. 2005; 366:1512–1514. [PubMed: 16257330]

Heidenreich PA, Kapoor JR. Radiation induced heart disease: systemic disorders in heart disease. Heart. 2009; 95:252–958. [PubMed: 19144884]

Imamura T, Dubin A, Moore W, Tanaka Rm Travis J. Induction of vascular permeability enhancement by human tryptase: dependence on activation of prekallikrein and direct release of bradykinin from kininogens. Lab Invest. 1996; 74:861–870. [PubMed: 8642782]

Jaworski C, Mariani JA, Wheeler G, Kaye DM. Cardiac complications of thoracic irradiation. J Am Coll Cardiol. 2013; 61:2319–2328. [PubMed: 23583253]

Jones SP, Bolli R. The ubiquitous role of nitric oxide in cardioprotection. J Molec Cell Cardiol. 2006; 40:16–23. [PubMed: 16288777]

Keefe DL. Trastuzumab-associated cardiotoxicity. Cancer. 2003; 2002; 95:1592–1600. First published: Erratum: Cancer. 2003;97:1136. [PubMed: 12237930]

Kim NN, Villegas S, Summerour SR, Villarreal FJ. Regulation of cardiac fibroblast extracellular matrix production by bradykinin and nitric oxide. J Mol Cell Cardiol. 1999; 31:456–466.

Larsen RL, Jakacki RI, Vetter VL, Meadows AT, Silber JH, Barber G. Electrocardiographic changes and arrhythmias after cancer therapy in children and young adults. Am J Cardiol. 1992; 70:73–77. [PubMed: 1615874]

Leppä S, Saffrich R, Ansorge W, Bohmann D. Differential regulation of c-Jun by ERK and JNK during PC12 cell differentiation. EMBO J. 1998; 17:4404–4413. [PubMed: 9687508]

Marceau F, Bachvarov DR. Kinin receptors. Clin Rev Allergy Immunol. 1998; 16:385–401. [PubMed: 9926287]

Marceau F, Lussier A, Regoli D, Giroud JP. Pharmacology of kinins: their relevance to tissue injury and inflammation. Gen Pharmacol. 1983; 14:209–229. [PubMed: 6132853]

Martinez FO, Gordon S. The M1 and M2 paradigm of macrophage activation: time for reassessment. F1000Prime Rep. 2014; 6:13. [PubMed: 24669294]

Mount PF, Kemp BE, Power DA. Regulation of endothelial and myocardial NO synthesis by multi-site eNOS phosphorylation. J Mol Cell Cardiol. 2007; 42:271–279. [PubMed: 16839566]

Nellessen U, Zingel M, Hecker H, Bahnsen J, Borschke D. Effects of radiation therapy on myocardial cell integrity and pump function: which role for cardiac biomarkers? Chemother. 2010; 56:147–152.

Regoli D, Plante GE, Gobeil F. Impact of kinins in the treatment of cardiovascular diseases. Pharmacol Ther. 2012; 135:94–111. [PubMed: 22537664]

Rose BA, Force T, Wang Y. Mitogen-activated protein kinase signaling in the heart: angels versus demons in a heart-breaking tale. Physiol Rev. 2010; 90:1507–1546. [PubMed: 20959622]

Sridharan V, Sharma SK, Moros EG, Corry PM, Tripathi P, Lieblong BJ, Guha C, Hauer-Jensen M, Boerma M. Effects of radiation on the epidermal growth factor receptor pathway in the heart. Int J Radiat Biol. 2013; 89:539–547. [PubMed: 23488537]

Sridharan V, Tripathi P, Sharma SK, Moros EG, Corry PM, Lieblong BJ, Kaschina E, Unger T, Thöne-Reineke C, Hauer-Jensen M, Boerma M. Cardiac inflammation after local irradiation is influenced by the kallikrein-kinin system. Cancer Res. 2012; 72:4984–4992. [PubMed: 22865451]

Tsutsumi Y, Matsubara H, Masaki H, Kurihara H, Murasawa S, Takai S, Miyazaki M, Nozawa Y, Ozono R, Nakagawa K, Miwa T, Kawada N, Mori Y, Shibasaki Y, Tanaka Y, Fujiyama S, Koyama Y, Fujiyama A, Takahashi H, Iwasaka T. Angiotensin II type 2 receptor overexpression activates the vascular kinin system and causes vasodilation. J Clin Invest. 1999; 104:925–935. [PubMed: 10510333]

Wang X, Wei M, Kyykasjärvi P, Laurikka J, Rinne T, Moilanen E, Tarkka M. The anti-inflammatory effect of bradykinin preconditioning in coronary artery bypass grafting (bradykinin and preconditioning). Scand Cardiovasc J. 2009; 43:72–79. [PubMed: 18609065]

Wethal T, Lund MB, Edvardsen T, Fosså SD, Pripp AH, Holte H, Kjekshus J, Fosså A. Valvular dysfunction and left ventricular changes in Hodkin's lymphoma survivors: a longitudinal study. Br J Cancer. 2009; 101:575–581. [PubMed: 19623176]

Windak R, Müller J, Felley A, Akhmedov, Wagner E, Pedrazzini T, Sumara G, Ricci R. The AP-1 transcription factor c-Jun prevents stress-imposed maladaptive remodeling of the heart. PLoS One. 2013; 8:e73294. [PubMed: 24039904]

Wirth K, Hock FJ, Albus U, Linz W, Alpermann HG, Anagnostopoulos H, Henke St, Breipohl G, König W, Knolle J, Schölkens BA. Hoe 140 a new potent and long acting bradykinin-antagonist: *in vivo* studies. Br J Pharmacol. 1991; 102:774–777. [PubMed: 1364852]

Wonnacott S. The paradox of nicotinic acetylcholine receptor upregulation by nicotine. Trends Pharmacol Sci. 1990; 11:216–219. [PubMed: 2200178]

Xu J, Carretero OA, Zhu L, Shesely EG, Rhaleb N, Dai X, Wang L, Yang JJ, Yang X. Protective role of AT_2 and B_1 receptors in kinin B_2-receptor-knockout mice with myocardial infarction. Clin Sci. 2013; 124:87–96. [PubMed: 22849668]

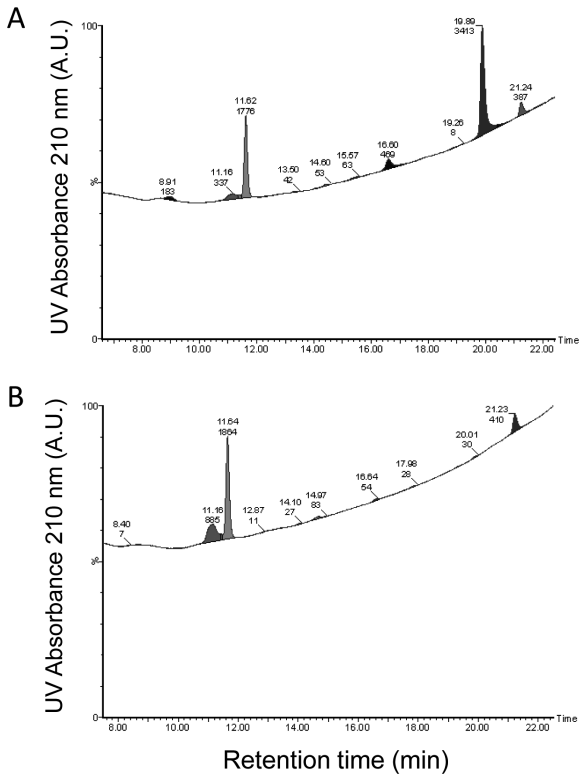

Figure 1.

HOE-140 showed high chemical stability in 0.9% saline as demonstrated using HPLC with UV detection. (A) Representative reversed-phase HPLC chromatogram of HOE-140 freshly dissolved in saline vehicle. (B) Representative reversed-phase HPLC chromatogram of HOE-140 after 18 days incubation in an osmotic minipump at 37°C. The peak at 11.6 minutes corresponds to elution of HOE-140.

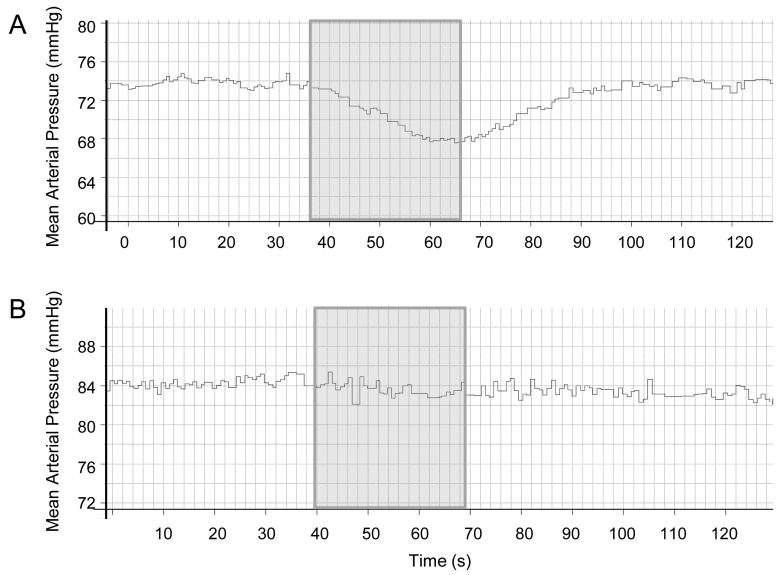

Figure 2.

HOE-140 blocked the hypotensive response to BK. Shaded boxes indicate intravenous infusion of 0.3 μg/kg BK over 30 sec. Horizontal axis ticks denote 10 sec intervals. (A) Representative MAP trace of a rat treated with saline vehicle for 35 days via osmotic minipump. (B) Representative MAP trace of a rat treated with 0.5 mg/kg/day HOE-140 for 32 days via osmotic minipump. Treatment with HOE-140 blocked the hypotensive response to BK.

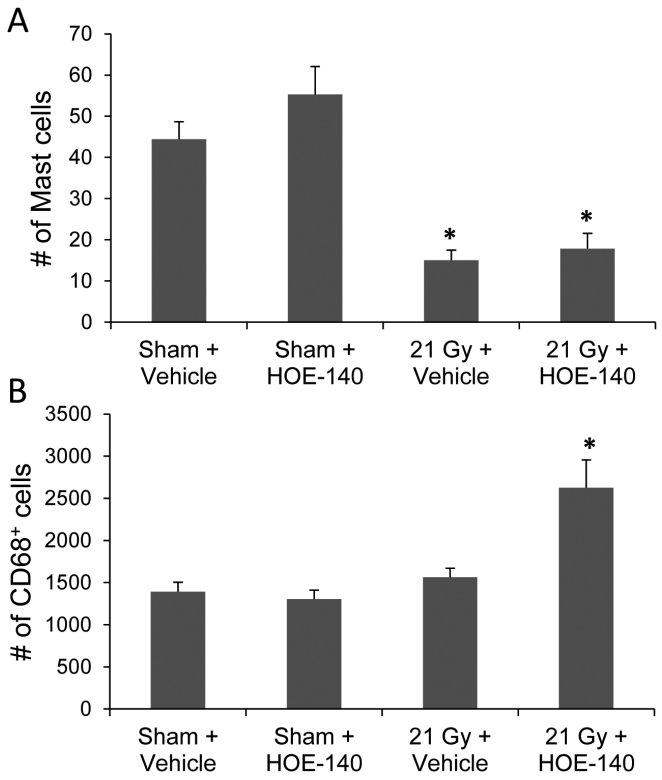

Figure 3.

(A) Radiation caused a four-fold decrease in the number of mast cells in the heart, while HOE-140 treatment had no effect on mast cell numbers. (B) HOE-140 treatment caused an increase in myocardial numbers of $CD68^+$ cells in animals that received local heart irradiation. Values are average ± SEM, n=13, 7, 7, 6. *$p<0.05$ compared to sham-irradiated group.

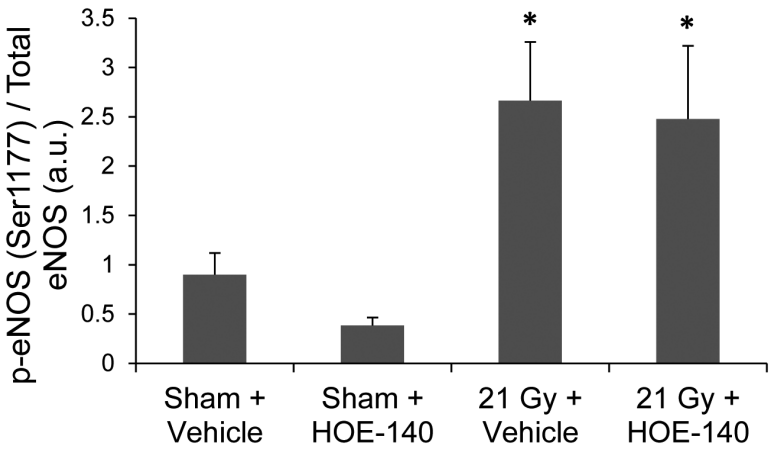

Figure 4.

Radiation caused a 2.5-fold increase in eNOS phosphorylation, while HOE-140 treatment did not inhibit eNOS phosphorylation in sham-irradiated or irradiated animals. Values are average ± SEM, n=13, 7, 7, 6. *p<0.05 compared to sham-irradiated group.

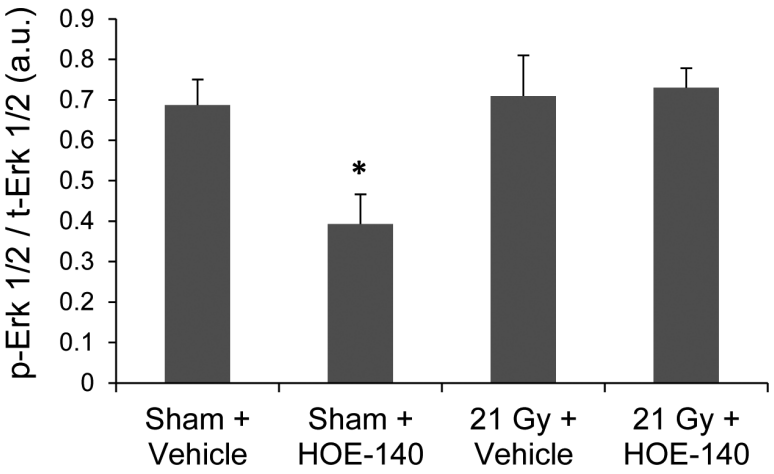

Figure 5.

HOE-140 treatment caused a two-fold reduction in Erk 1/2 phosphorylation in sham-irradiated animals, while HOE-140 treatment did not affect cardiac Erk 1/2 phosphorylation in animals which received local heart irradiation. Values are average ± SEM, n=13, 7, 7, 6. *p<0.05 compared to sham-irradiated.

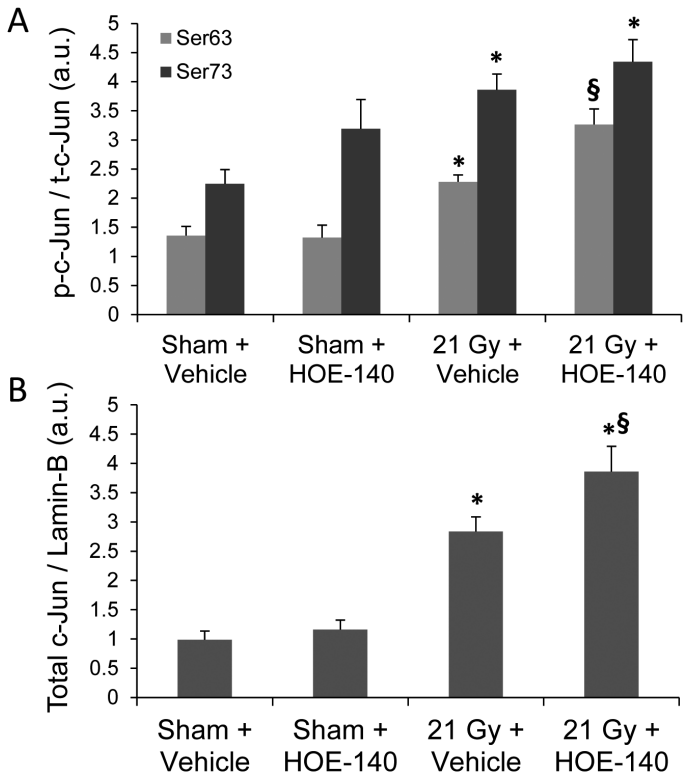

Figure 6.

HOE-140 treatment and local heart irradiation increased phosphorylation and nuclear translocation of c-Jun. (A) In total left ventricular homogenates, radiation caused an increase in phosphorylation of c-Jun at both the Ser63 and Ser73 residues, and HOE-140 treatment caused a further increase in c-Jun phosphorylation at Ser63. (B) In left ventricular nuclear extracts, radiation caused an approximately 2.5-fold increase in total c-Jun nuclear translocation. HOE-140 treatment caused a further increase in irradiated animals, while it had no effect in sham animals. Values are average ± SEM, n=13, 7, 7, 6. *$p<0.05$ compared to sham-irradiated group. §$p<0.05$ compared to irradiated group.